ELSEVIER

Polymer 41 (2000) 8681–8687

polymer

www.elsevier.nl/locate/polymer

Aggregation behavior of poly(*N*,*N*-diethylacrylamide) in aqueous solution

M. Itakura, K. Inomata, T. Nose*

Department of Polymer Chemistry, Tokyo Institute of Technology, 2-12-1, O-okayama, Meguro-ku, Tokyo 152-8552, Japan

Received 24 December 1999; received in revised form 4 March 2000; accepted 31 March 2000

Abstract

Aggregation behavior of poly(*N*,*N*-diethylacrylamide) (PDEA) in dilute aqueous solution has been studied by using the static and dynamic light scattering. It has been demonstrated that PDEA is not molecularly dissolved in water but forms molecular aggregates below the cloud point in one phase region. The association number of aggregates is of the order of 100, and the aggregate is suggested to be like a swollen micro-gel. The aggregation does not come from difficulty of dissolving a frozen structure in solid state, but the aggregates are also formed in solution starting from aggregation-free state by changing the solvent quality. The detailed aggregate size and structure depend on the dissolution process of the solid sample in making the solution. Once the aggregate is formed, it is stable, and does not change its association number and dimension for a long time. But, the association number may change with temperature and depends on thermal history.

Keywords: Poly(*N*,*N*-diethylacrylamide); Light scattering; Aggregation behavior

1. Introduction

N-substituted acrylamide polymers have attracted much attention as water soluble polymers from both scientific and practical interests [1–11]. Especially, solution and gel properties of poly(*N*-isopropylacrylamide) have been investigated most extensively [3–11]. Recently, attention has also been paid for poly(*N*,*N*-diethylacrylamide) (PDEA) as a water soluble polymer, which becomes insoluble above room temperature [12–14]. Idziak et al. have reported that the cloud point of PDEA aqueous solution is about 35°C, depending on the heating rate [12], while Freitag et al. have found that the cloud point depends on polymerization method of PDEA [13]. On the other hand, Ilavsky and coworkers have investigated PDEA gels by various experimental techniques, and demonstrated that the gels are temperature-sensitive [15–18].

In these previous studies, it has been presumed that the PDEA is molecularly dissolved in water. However, to our knowledge, properties of PDEA aqueous solution have not been studied extensively as yet, and it has not been confirmed experimentally whether PDEA molecules are molecularly dispersed in water or not.

Recently, by means of light scattering technique, we have found that PDEA is not molecularly dispersed but forms aggregates in water. In this study, we investigate detailed aqueous solution properties of PDEA by static and dynamic light scattering to reveal the aggregation behavior of PDEA in water.

2. Experiments

2.1. Materials

PDEAs were prepared by anionic polymerization with two different initiators. One has a diphenyl group at the chain end, denoted as f-PDEA, and the other has no diphenyl group, denoted as n-PDEA. Their chemical structures and molecular weights are shown in Fig. 1 and listed in Table 1, respectively. The tacticity in triad level was measured by ^{13}C nuclear magnetic resonance [19] to be $mm = 7\%$, $mr = 89\%$, and $rr = 4\%$ for f-PDEA, and $mm = 11\%$, $mr = 83\%$, and $rr = 6\%$ for n-PDEA. The results show that the tacticities of both samples are heterotactic, not obeying the Bernoullian statistics. The cloud points of f-PDEA and n-PDEA aqueous solutions are around 30 and 38°C, respectively.

Water was de-ionized and then filtered by Milli-Q Jr. (Millipore Co.) before use. The resistivity of the water was kept at about 18.3 MΩcm.

* Corresponding author. Tel.: +81-3-5734-2132; fax: +81-3-5734-2888.

E-mail address: tnose@polymer.titech.ac.jp (T. Nose).

0032-3861/00/$ - see front matter
PII: S0032-3861(00)00267-6

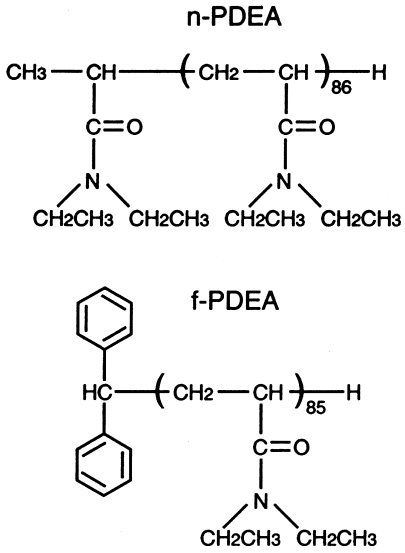

Fig. 1. Chemical structures of f-PDEA and n-PDEA samples.

2.2. Light scattering measurements

The light scattering apparatus was a specially designed one with an Ar-ion laser operating at the wavelength of 488 nm as the light source. The correlator used in the dynamic light scattering was a Multiple-Tau Digital Correlator, ALV-5000. The temperature was controlled within ±0.01°C. Details of the light scattering spectrometer have been described elsewhere [20].

The excess Rayleigh ratio $R_{vv}(\theta)$ was calculated from the measured excess scattered intensity as a function of the scattering angle θ. Since the extrapolation to the dilute limit was not available because of aggregation, we have evaluated the apparent molecular weight M_{wapp} and apparent radius of gyration R_{gapp} without the extrapolation, which are defined as

$$M_{wapp} = \frac{R_{vv}(0)}{KC} \tag{1}$$

$$R_{gapp}^2 = \frac{3\lambda_0^2 M_w(\text{initial slope})}{16\pi^2 n^2} \tag{2}$$

where the constant K is given by $K = 4\pi^2 n^2 (\partial n/\partial C)^2/(N_A \lambda_0^4)$, with n being the refractive index of the solvent, N_A the Avogadro constant, $(\partial n/\partial C)$ the refractive index increment, and λ_0 the wavelength of the incident beam in vacuum. The concentration C is in weight per volume of solution. $KC/R_{vv}(0)$ and (initial slope) are the intercept and the initial slope of $KC/R_{vv}(\theta)$ vs $\sin^2(\theta/2)$ plots at a finite concentration. The refractive index increment was measured by a differential refractometer as a function of temperature t, and is described by the following equation:

$$(\partial n/\partial C)/(\text{ml/g}) = 0.1905 - 0.00064(t/°\text{C})$$

The apparent particle scattering factor $P_{app}(q)$ was also calculated by

$$P_{app}(q) = R_{vv}(q)/R_{vv}(0) \tag{3}$$

where the momentum transfer q is given by $q = (4\pi n/\lambda_0)\sin(\theta/2)$.

The correlation function of the electric field obtained from the auto-correlation function of the scattered light intensity exhibited a unimodal decay and allowed us to obtain the decay rate Γ and the variance μ_2/Γ^2 by the second-order cumulant method [21]. The diffusion coefficient, D, was calculated by $D = \Gamma/q^2$ and then was extrapolated to $q = 0$, if D depended on q; otherwise, D at $\theta = 30°$ was regarded as those at $q = 0$. The obtained D was transformed to the hydrodynamic radius R_h by the Einstein–Stokes equation

$$R_h = \frac{kT}{6\pi\eta_0 D} \tag{4}$$

where k, T and η_0 are the Boltzmann constant, absolute temperature and solvent viscosity, respectively. Similar to the static properties, we evaluated the hydrodynamic radius without extrapolating to dilute limit, which is here referred to as the apparent hydrodynamic radius R_{happ}.

2.3. Shear viscosity measurements

Shear viscosity (η) of PDEA aqueous solution was measured by the rolling ball method. The viscometer consisted of a glass capillary tube of 1.8 mm inner diameter and a bearing ball of 1.3 mm diameter. The temperature was regulated at ±0.05°C in a water bath. The value of η was evaluated using the modified Sage's relation. Details of the measurements have been described elsewhere [22].

2.4. Preparation of sample solutions

Powder of PDEA was dissolved in water cooled in an ice bath to make a stock aqueous solution of 0.3 wt%. The solution was filtered through a Millipore filter of pore size of 0.2 μm into a dust-free light scattering glass tube, and then an appropriate amount of solvent water was filtered directly into the tube to obtain the sample solution of desired concentration. The sample glass tube was flame-sealed under mild vacuum, and was left at room temperature for one night to equilibrate the solution. For testing the effect of freezing of aggregation in solid PDEA formed before dissolution, we also made a PDEA solution by using a good solvent and subsequently replaced the good solvent with

Table 1
Characteristics of PDEA samples

Sample code	M_n[a]	M_w/M_n[a]	Cloud point (°C)[b]
f-PDEA	10 100	1.15	30
n-PDEA	11 000	1.10	38

[a] Measured by SEC with DMF as solvent and poly(methyl methacrylate) standards.
[b] Heating rate of 1°C/min.

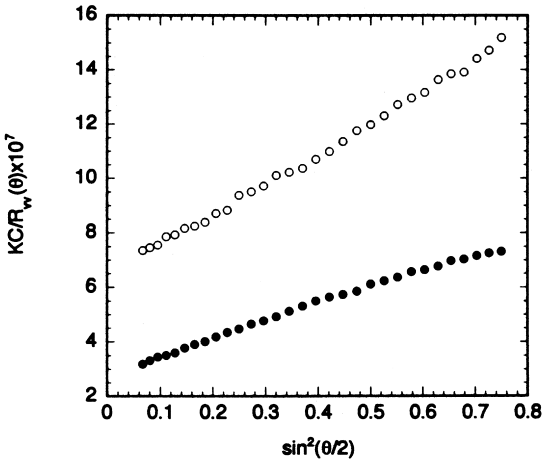

Fig. 2. Zimm-type plots of scattered light intensity for: f-PDEA(●); and n-PDEA(○) aqueous solutions at 20°C. The concentration is 0.3 wt% for both f-PDEA and n-PDEA.

water by the following procedure. First, PDEA was dissolved in tetrahydrofurane (THF) to make a solution, followed by adding water to the solution, and it was fractionally distilled under reduced pressure to make more concentrated but less THF content solution. Then we added water again, and distilled the solvent. We repeated this process, and finally obtained a purely aqueous solution. No trace of THF was detected by gas chromatography. The obtained solution was further concentrated by evaporation to make the highest concentration in the present light scattering experiments. Dilution with water was carried out in the same manner as mentioned above to prepare sample solutions of the desired concentration.

3. Results and discussion

3.1. Aggregations

Examples of angular dependencies of the scattered light intensity for f-PDEA and n-PDEA aqueous solutions at 20°C are shown in Fig. 2 as Zimm-type plots, and apparent molecular weights and radii of gyration evaluated from these plots are listed in Table 2, along with the results of dynamic light scattering. M_{wapp}s are more than 100 times larger than those of the PDEA samples measured by size exclusion chromatography (SEC) in *N*,*N*-dimethylformamide (DMF), and the dimensions are several ten nm, much larger than the expected dimensions of an isolated PDEA molecule called as unimer here. These results indicate that both f-PDEA and n-PDEA form aggregate with association numbers of the order of 100 irrespective of the presence of diphenyl end group. Similar results were obtained for the concentration ranging from 0.001 to 0.3 wt%, showing the formation of aggregates with similar sizes even in a very dilute solution over the whole range of experimental concentration. It should be noted here that the quantitative results of light scattering change from solution to solution prepared in different conditions, exhibiting poor reproducibility, although the association number and the dimension of aggregates have always the same orders of magnitude. This suggests the possibility that there still remains some aggregates formed in bulk before dissolving in water.

In Table 3 are listed the apparent molecular weight M_{wapp} for PDEA in THF solution. The values are a couple of times of those of unimers, indicating no appreciable formation of aggregates in THF. Table 4 summarizes the light scattering results for the PDEA aqueous solution prepared from the THF solution. M_{wapp}s are of the order of 10^6, indicating the formation of aggregates with an association number of the order of 100. The aggregates have the dimension of about 100 nm. Therefore it is concluded that PDEA forms aggregates in aqueous solution from almost molecularly dispersed state, which have M_{wapp} similar to those of the aggregates formed in the directly prepared aqueous solution from the PDEA powder. The difference in dimension between the differently prepared solutions is within the reproducibility observed in the solutions prepared directly. The aggregation observed is not due to incomplete dissolution process of bulk PDEA into water, but PDEA can form stable aggregates in pure water by intermolecular associations. To our knowledge, the presence of molecular association in PDEA aqueous solution has not been reported before.

3.2. Time dependence of aggregates

Fig. 3 shows changes in the scattered light intensity $I/I_{Benzene}$, where $I_{Benzene}$ is the scattered light intensity of pure benzene for standard, at an angle of 30° (left axis) and in R_{happ} (right axis) with time at a fixed temperature of 20°C. No significant changes in $I/I_{Benzene}$ and R_{happ} are found for 19 days. This indicates that the aggregates are stable in solution showing no changes in the association number and the dimension once they are formed.

3.3. Temperature dependence of aggregates

In Fig. 4 are shown M_{wapp}, R_{gapp} and R_{happ} as functions of temperature for n-PDEA aqueous solution of 0.3 wt% under

Table 2
Numerical results of light scattering measurements for PDEA aqueous solutions at 20°C

Sample code	Concentration (g/g)	M_{wapp}	R_{gapp} (nm)	R_{happ}(nm)	R_{gapp}/R_{happ}	μ_2/Γ^2
f-PDEA	3.36×10^{-3}	3.7×10^6	79	60	1.32	0.17
n-PDEA	3.33×10^{-3}	1.4×10^6	37	50	0.74	0.14

Table 3
Numerical results of the light scattering measurements for PDEA/THF systems at 20°C

Sample code	Concentration (g/g)	M_{wapp}
f-PDEA	1.03×10^{-2}	3.2×10^4
n-PDEA	1.04×10^{-2}	4.2×10^4

repeated heating and cooling processes. Here the thermal history was as follows: the solution was first heated from 20 to 35°C, standing at each experimental temperature for 2 h (run-1). The solution was opaque when the temperature reached at 35°C, then it became transparent again by annealing at 35°C for 3 days. After confirming the transparency, the solution was cooled down to 20°C, standing at each experimental temperature for 2 h (run-2). The last run of heating (run-3) was performed after leaving the solution at 20°C overnight and subsequently the solution was heated in the same manner of run-1. In any temperature-change processes M_{wapp} increases with increasing temperature, and more sharply increases as the cloud point was approached. On the other hand, with increasing temperature, the dimension of aggregates, observed as R_{gapp} and R_{happ}, decreases around 30°C once and then abruptly increases near the cloud point. This indicates the occurrence of a slight shrinkage of the aggregation particle, suggesting that the polymer chains forming the aggregate shrink owing to the decrease in the solvent quality with increasing temperature. The decrease in the solvent quality to PDEA chains eventually results in making the solution cloudy.

It is noteworthy that the cloud point observed here is not an indication of the onset of usual phase separation since the cloudy solution becomes transparent again on waiting for a long time at that temperature, but there was no trace of precipitation observed with the solution still giving a high scattered light intensity. It turns out that the associations of PDEA bringing about the very large aggregates take place below and even near the cloud point without showing the phase separation. Therefore the association may not be related directly to the phase separation.

As seen in Fig. 4, the larger aggregates grow first by heating up to the cloud point, and they are not decomposed by cooling and further repeated heating, exhibiting an irreversible change with temperature. That is, the structure of aggregates once formed at higher temperatures is fairly stable and is not decomposed any more by temperature change below the cloud point.

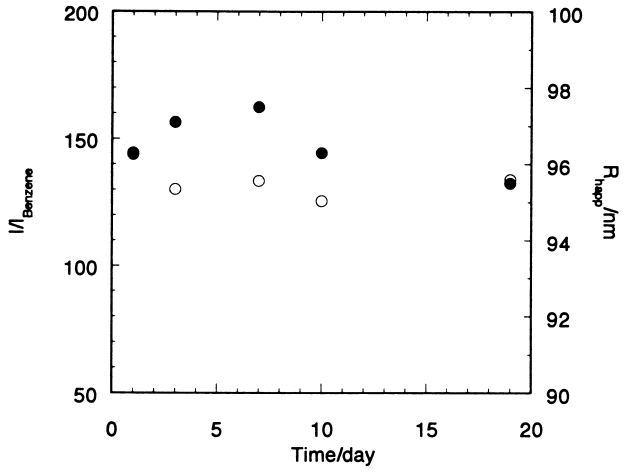

Fig. 3. Time dependencies of the scattered light intensity $I/I_{Benzene}$ (○) at $\theta = 30°$ and R_{happ} (●) at the fixed temperature of 20°C for n-PDEA aqueous solution of 0.3 wt% ($I_{Benzene}$ is the scattered light intensity of benzene for standard).

Fig. 5 presents the temperature dependence of specific viscosity $\eta_{sp} = (\eta - \eta_0)/\eta_0$, where η_0 and η are the shear viscosity of solvent and solution, respectively, for PDEA aqueous solution of 0.3 wt%. The temperature dependence of η_{sp} is complex but weaken up to 35°C, where η_{sp} starts increasing abruptly, immediately followed by non-smooth rolling of the steel ball in the viscometer capillary, which may be a sign of appreciable heterogeneity in the polymer solution. No indication of phase separation was observed in viscosity lower than 35°C. This may support the above interpretation for the light scattering results. Decrease in η_{sp} with the increase of temperature below 30°C may be due to the shrinkage of aggregate, and the followed increase may come from increasing number of aggregates, the effect of which dominates that of the shrinkage.

Thermal history effects were also observed by giving other temperature history. An aqueous solution prepared directly from the PDEA powder was kept at 5°C, and this solution was sometimes heated to 20–35°C and again cooled to 5°C for annealing. After this temperature history, the aggregation behavior was different from those mentioned above, where the shrinkage of aggregates near the cloud point was not observed.

It should be noted here again that the observed aggregates

Table 4
Numerical results of the light scattering measurements for the PDEA aqueous solutions prepared from the THF solution at 20°C

Sample code	Concentration (g/g)	M_{wapp}	R_{gapp} (nm)	R_{happ} (nm)	R_{gapp}/R_{happ}	μ_2/Γ^2
f-PDEA	3.1×10^{-3}	1.9×10^6	134	77	1.74	0.23
n-PDEA	3.2×10^{-3}	3.2×10^6	112	96	1.17	0.07

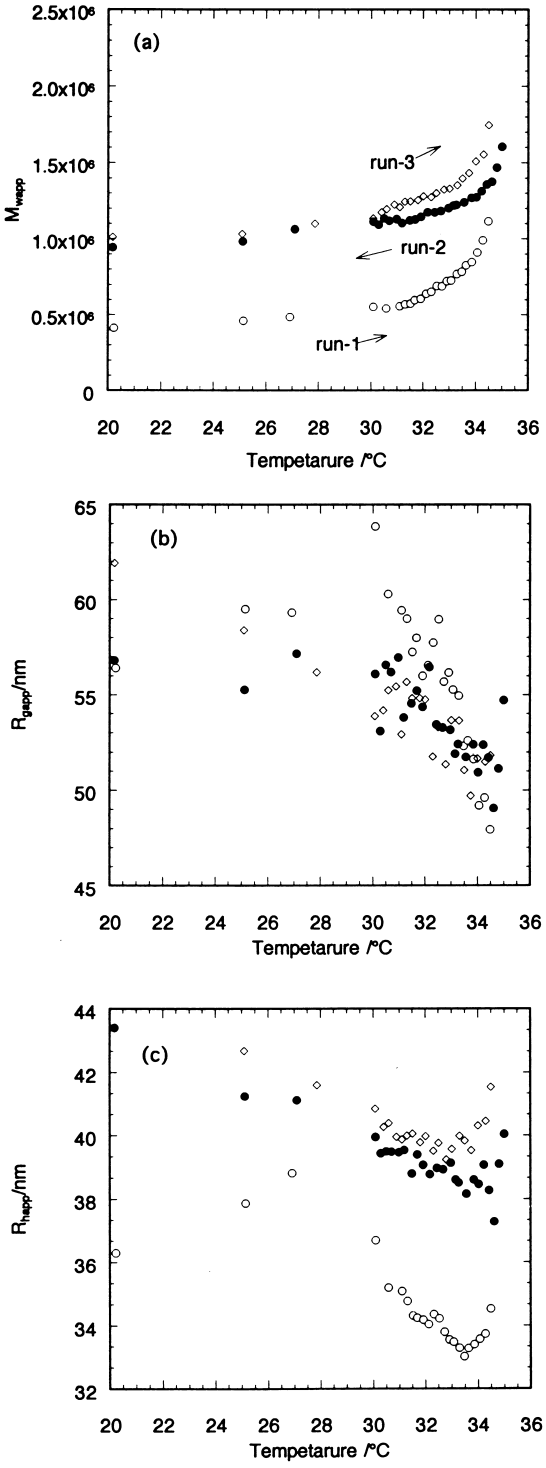

Fig. 4. Changes of: (a) M_{wapp}, (b) R_{gapp}; and (c) R_{happ} with temperature for n-PDEA aqueous solutions of 0.3 wt% under repeated heating and cooling processes. (○) the first heating (run-1); (●) cooling (run-2); (◇) the second heating (run-3). Details of thermal history are described in the text.

are not the equilibrium ones, and the detailed behaviors of aggregates are not reproducible, but change from sample solution to sample solution, and depend on thermal histories of solution. Therefore, the above-mentioned behaviors are not observed always.

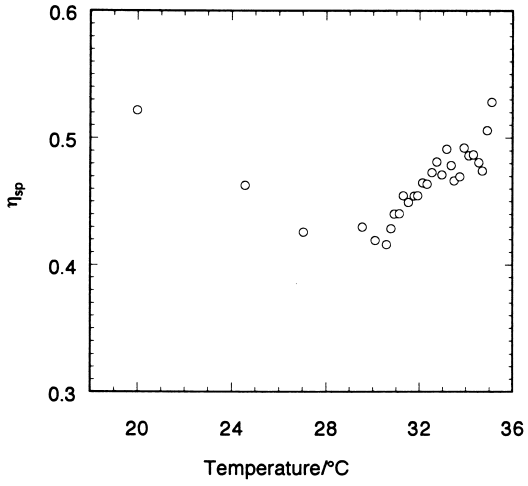

Fig. 5. Temperature dependency of specific viscosity $\eta_{sp} = (\eta - \eta_0)/\eta_0$ for n-PDEA aqueous solution of 0.3 wt%.

3.4. Structure of aggregates

Fig. 6 shows the observed particle scattering factors along with the theoretical ones for typical particle shapes. It is difficult, from this figure, to judge a likely particle shape since the experimental range of $R_{gapp}q$ is not wide enough and the possible presence of a particle size distribution. An example of $R_{gapp}q$-dependence of the diffusion coefficient, D, is shown in Fig. 7. Even in the range of $R_{gapp}q < 1$, D increases slightly with increasing q, reflecting the presence of polydispersity of particle size. The anisotropy of the particle shape cannot be deduced from the $R_{gapp}q$-dependence because of the limited $R_{gapp}q$ range and polydispersity. The polydispersity index μ_2/Γ^2 of dynamic scattering, as listed in Table 2 for examples, ranges from 0.1 to 0.2, which is somewhat larger than those of the usual block-copolymer micelles formed in a selective solvent.

In Fig. 8 are plotted the ratio of R_{gapp}/R_{happ}, another index for the particle shape, against M_{wapp} for the PDEA aqueous solutions of different concentrations at different temperatures. The index ranges from 1 to 1.5, and is almost a constant value of about 1.2 at a larger M_{wapp}s. This value is larger than that for the solid sphere (0.774), comparable to that of the star-shaped polymer (1.1–1.5), and less than those for a random-coil (1.5–1.8) and rod-like molecule (5 at the thin and long limit) [23]. Considering that the index is determined by the segment density distribution in a particle, a likely structure of the aggregate is expected from the index to be a sphere (or a slightly elongated one) with a diffused surface boundary.

To see the magnitude of segment density in the particle, we evaluated the average segment density (or concentration) ϕ_{aggr} in volume fraction by the following equation:

$$\phi_{aggr} = \frac{M_{wapp}}{(4\pi/3)(R_{happ})^3 N_A \rho_{polym}} \quad (5)$$

Here, ρ_{polym} is the polymer density. The values of ϕ_{aggr}

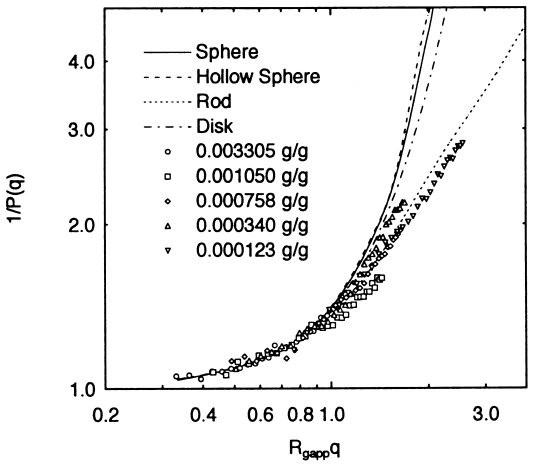

Fig. 6. Particle scattering factors for n-PDEA aqueous solutions of different concentrations as indicated, along with theoretical ones for some simple shapes.

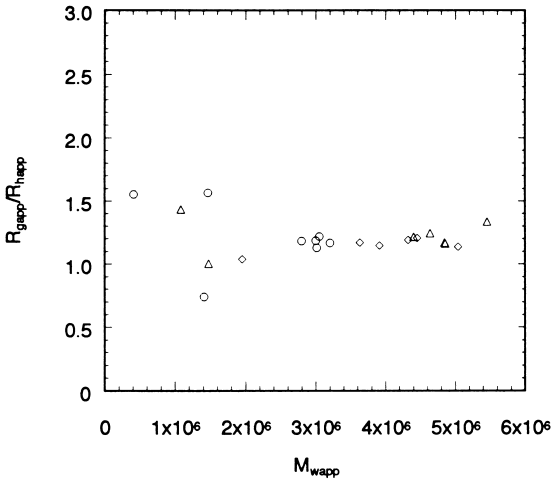

Fig. 8. Plots of R_{gapp}/R_{happ} against M_{wapp} for n-PDEA aqueous solutions of different concentrations at 20°C. Concentration: (◇), 0.07 wt%; (△), 0.1 wt%; (○), 0.3 wt%.

thus calculated for aggregates formed under different conditions are plotted against M_{wapp} in Fig. 9. The values are of the order of 10^{-3}, showing no systematic dependence on M_{wapp} and being almost constant, about 0.002, at larger M_{wapp}s. These values are comparable to or a little smaller than those for the random-coil polymers in solution, for example, 0.0041–0.014 for poly(*N*-isopropylacrylamide) with the molecular weight ranging from 1.33×10^5 to 1.59×10^6 [1,8].

Summarizing the above discussion on the structure, we can estimate the aggregate structure to be like a micro-gel with low segment density, and the structures of larger aggregates (at higher M_{wapp}) are similar to each other, having $R_{gapp}/R_{happ} = 1.2$ and $\phi_{aggr} = 0.002$.

To form the aggregates with the above-estimated structure before the cloud point shows up with increasing attractive segment interactions, the interactions yielding the associate should not be the ones uniformly distributed over the chain, but must be a specific pin-point interaction making segmental bondings acting as cross-linking points. The interaction possibly originates from an irregular microstructure of the polymer, such as stereo-regularity, which interplays with water and influences the solubility in aqueous solution. Actually, it has been reported that the solubility of N-substituted acrylamide polymers depends on the stereo-regularity [19].

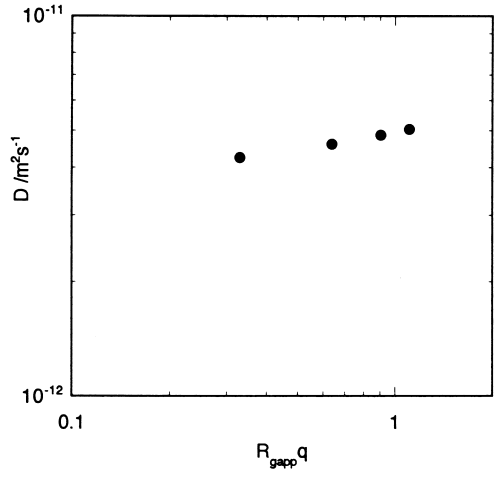

Fig. 7. $R_{gapp}q$-dependency of diffusion coefficient, *D*, for n-PDEA aqueous solution of 0.3 wt% at 20°C.

4. Conclusions

1. Poly(*N*,*N*-diethylacrylamide), irrespective of the presence of diphenyl end groups, is not molecularly dissolved in water, but forms aggregates in one-phase aqueous solution below the cloud point.

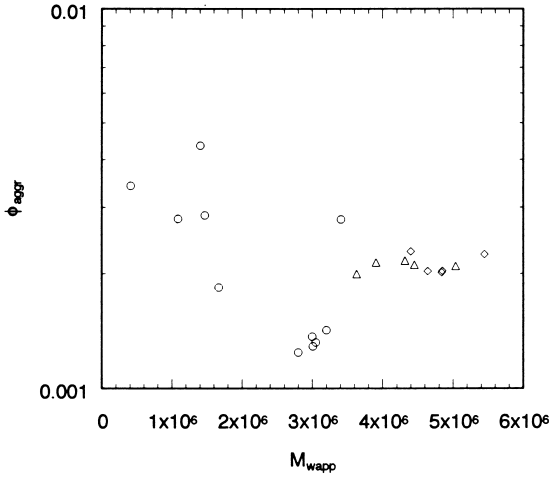

Fig. 9. The values of ϕ_{aggr} calculated by Eq. (5) plotted as a function of M_{wapp} for aggregates in n-PDEA aqueous solution at 20°C formed under various conditions. Concentration: (◇), 0.07 wt%; (△), 0.1 wt%; (○), 0.3 wt%.

2. The aggregates are not present as a result of maintaining of the solid state structure, but formed by molecular associations in solution.
3. Once the aggregates are formed, they are not easily decomposed, but grow as the cloud point is approached, so that the aggregates are rather stable but not at equilibrium.
4. The aggregates are like a swollen micro-gel, with the association number being of the order of 100 and the dimension being several ten nm.

Acknowledgements

The authors greatly appreciate Professor Seiichi Nakahama of Tokyo Institute of Technology for kindly providing PDEA samples. This work was partly supported by a Grant in Aid for Scientific Research (No. 10305066) from the Ministry of Education, Science, Sports and Culture of Japan.

References

[1] Ito D, Kubota K. Macromolecules 1997;30(25):7828–34.
[2] Trossarelli L, Meirone M. J Polym Sci 1962;57:445–52.
[3] Yamamoto I, Iwasaki K, Hirotsu S. J Phys Soc Jpn 1989;58(1):210–5.
[4] Schild HG, Tirrell DA. J Phys Chem 1990;94(10):4352–6.
[5] Meewes M, Ricka J, de Silva M, Nyffenegger R, Binkert Th. Macromolecules 1991;24(21):5811–6.
[6] Fujishige S. Polym J 1987;19(3):297–300.
[7] Fujishige S, Kubota K, Ando I. J Phys Chem 1989;93(8):3311–3.
[8] Kubota K, Fujishige S, Ando I. J Phys Chem 1990;94(12):5154–8.
[9] Heskins M, Guillet JE. J Macromol Sci, Chem 1968;A2(8):1441–55.
[10] Wu C, Zhou S. Macromolecules 1995;28(24):8381–7.
[11] Zeng F, Zheng X, Tong Z. Polymer 1998;39(5):1249–51.
[12] Idziak I, Avoce D, Lessard D, Gravel D, Zhu XX. Macromolecules 1999;32(4):1260–3.
[13] Freitag R, Baltes T, Eggert M. J Polym Sci 1994;32:3019–30.
[14] Taylor LD, Creankowski LD. J Polym Sci, Polym Chem Ed 1975;13:2551–70.
[15] Hrouz J, Ilavsky M. Polym Bull 1989;22:271–6.
[16] Plestil J, Ostanesvich Y, Borbely S, Stejskal J, Ilavsky M. Polym Bull 1987;17:465–72.
[17] Plestil J, Ilavsky M, Pospisil H, Hlavata D. Polymer 1993;34(23):4846–51.
[18] Liptak J, Ilavsky M, Nedbal J. Polym Networks Blends 1995;5(1):55–61.
[19] Kobayashi M, Okuyama S, Ishizone T, Nakahama S. Macromolecules 1999;32(20):6466–77.
[20] Varma B, Fujita Y, Takahashi M, Nose T. J Polym Sci, Polym Phys Ed 1984;22:1781–97.
[21] Koppel DE. J Chem Phys 1972;57(11):4814–20.
[22] Miyashita N, Nose T. J Chem Phys 1998;108(10):4282–91.
[23] Burchard W. Makromol Chem, Macromol Symp 1998;18:1–35.